Estimating Mass of Inflatable Aerodynamic Decelerators Using Dimensionless Parameters

Jamshid A. Samareh*

NASA Langley Research Center

This paper describes a technique for estimating mass for inflatable aerodynamic decelerators. The technique uses dimensional analysis to identify a set of dimensionless parameters for inflation pressure, mass of inflation gas, and mass of flexible material. The dimensionless parameters enable scaling of an inflatable concept with geometry parameters (e.g., diameter), environmental conditions (e.g., dynamic pressure), inflation gas properties (e.g., molecular mass), and mass growth allowance. This technique is applicable for attached (e.g., tension cone, hypercone, and stacked toroid) and trailing inflatable aerodynamic decelerators. The technique uses simple engineering approximations that were developed by NASA in the 1960s and 1970s, as well as some recent important developments. The NASA Mars Entry and Descent Landing System Analysis (EDL-SA) project used this technique to estimate the masses of the inflatable concepts that were used in the analysis. The EDL-SA results compared well with two independent sets of high-fidelity finite-element analyses.

Nomenclature

A_{gore}	=	gore total area, m^2
$\bar{A}_{\text{gore}}$	=	ratio of total gore area over IAD area
A_{IAD}	=	IAD projected area, m^2
A_R	=	ratio of IAD projected area to total projected area
A_r	=	radial strap cross-sectional area, m^2
C_d	=	IAD drag coefficient
c	=	gore chord length, m
C_i	=	toroid center circumference, m
$\bar{C}$	=	dimensionless parameter for total toroid circumference
D_i	=	inner heat-shield diameter, m
D_o	=	IAD overall diameter, m
$\overline{D_o}$	=	dimensionless parameter for IAD overall diameter (D_o/L)
D_t	=	torus minor diameter, m
F_a	=	aerodynamic drag force, N
F_c	=	compression load due to aerodynamic drag force, N
$\bar{G}$	=	dimensionless parameter for inflation gas
g_e	=	Earth gravity, 9.81 m/s^2
h	=	IAD slanted height, m
I	=	number of radial straps
k	=	Kyser recovery factor
L	=	characteristic length, m (L is assumed to be 1 m in this paper)
L_r	=	length of radial strap, m
$\bar{L}_r$	=	dimensionless parameter for radial strap length

* Aerospace Research Engineer, Vehicle Analysis Branch, AIAA Associate Fellow.

Jamshid.A.Samareh@NASA.gov

m	=	IAD mass, kg
$\bar{m}$	=	IAD dimensionless mass
m_f	=	Mach number flag for IAD attachment angles (1 for supersonic, 2 for hypersonic)
m_{factor}	=	mass factor $(A_{\text{IAD}} C_d q_{\max})/g_e$), kg
M	=	gas molecular mass, kg/kmole
N	=	number of toroids
N_θ, N_ψ	=	gore linear stress, N/m
$p_{\min}$	=	torus minimum inflation gage pressure, Pa
$\bar{p}_{\min}$	=	dimensionless minimum inflation gage pressure
p_s	=	gore surface pressure
$q_{\max}$	=	maximum dynamic pressure, Pa
R	=	universal gas constant (J/kmole·K)
r_θ, r_ψ	=	minimum gore curvatures, m
S_i	=	toroid total surface area, m^2
$\bar{S}$	=	dimensionless parameter for total toroid surface area
t	=	material thickness, m
T	=	inflation gas temperature, K
V_i	=	toroid total volume, m^3
$\bar{V}$	=	dimensionless parameter for toroid total volume
β	=	fiber bias angle, deg
δ	=	material allowance strain, m/m
η	=	growth allowance
ζ	=	shape factor
θ	=	half-cone angle, deg
θ_c	=	constructed angle (same as θ), deg
θ_d	=	deflected angle, deg
θ_h	=	attachment angle at heat shield, deg
θ_t	=	attachment angle at torus, deg
ξ_t	=	ratio of torus diameter to IAD diameter (D_t/D_o)
ξ_i	=	ratio of inner heat-shield diameter to IAD diameter (D_i/D_o)
ρ	=	material density, kg/m^3
σ	=	material tensile yield stress, Pa
$\bar{\sigma}$	=	dimensionless parameter for material yield tensile stress

I. Introduction

THE current Mars entry, descent, and landing (EDL) systems are based on the technology that was developed under the Viking program.[1] Landing large payloads requires large aeroshells, and using Viking rigid-aeroshell technology is well beyond the limits of current and possibly future launch vehicle systems. An inflatable aerodynamic decelerator (IAD) aeroshell is a viable option for large payload delivery to the surface of planetary bodies with appreciable atmospheres. *Ballute* is another name for IAD that was coined by the Goodyear Company in the 1960s, and the name combines the words *balloon* and *parachute*. Rohrschneider and Braun[2] provide an excellent survey of IAD technology for aerocapture.

The IAD concept is a flexible and lightweight structure that can be efficiently packed in a launch vehicle. The IADs are tensioned structures that, when inflated, provide a large drag area. The IAD structural stiffness is primarily a function of the inflation pressure. The aerodynamic loads, coupled with the internal inflation pressure, result in distributed loads that require the IAD design to remain in tension (i.e., no wrinkling or buckling) to keep the overall structure in a stable mode.

Figure 1 shows several IAD concepts, including stacked toroids (IRDT, IRVE, MIAS), a hypercone/tension cone (Flare, Hypercone), trailing IAD, RDSI, and spars and rims concepts. All IAD concepts have several common elements: inflated toroid(s), gores, radial straps, rigid heat shields, payload adaptors, and thermal protection system (TPS). Reza et al.[3] provide a discussion of several IAD concepts.

Jamshid.A.Samareh@NASA.gov

Among the IADs shown in Fig. 1, the IRVE, the IRDT, and the Flare have been flown. The Inflatable Reentry Vehicle Experiment (IRVE) is a stacked-toroid concept that launched successfully in August of 2009. Hughes et al.[4] provides an overview of the IRVE design. The European Space Agency and the Russian Federation designed the Inflatable Reentry and Descent Technology (IRDT) concept to return payload to Earth from the International Space Station.[5] The IRDT's first flight test was in November of 1996; this test was unsuccessful due to a launch failure. The second flight was in February 2000; this flight was partially successful. After completing six orbits, the vehicle entered the Earth's atmosphere; however, a tear in the inflatable heat shield occurred during descent and caused an impact velocity that was higher than planned. The wreckage was recovered. Two additional launches of the IRDT-2 both ended in failure; this time the vehicle wreckage could not be located after the reentry.[†] Flare[6] was a Japanese flight vehicle that consisted of a blunt capsule, a frustum-shaped membrane with a 45-deg cone angle, and a deployable outer frame. The membrane aeroshell was made of Zylon textile that was selected for its high heat resistance and strength. In August 2004, the aeroshell was mounted under a balloon gondola and released at an altitude of 39 km. This flight test demonstrated the aerodynamic capability of the flare-type thin-membrane aeroshell for an atmospheric-entry vehicle.

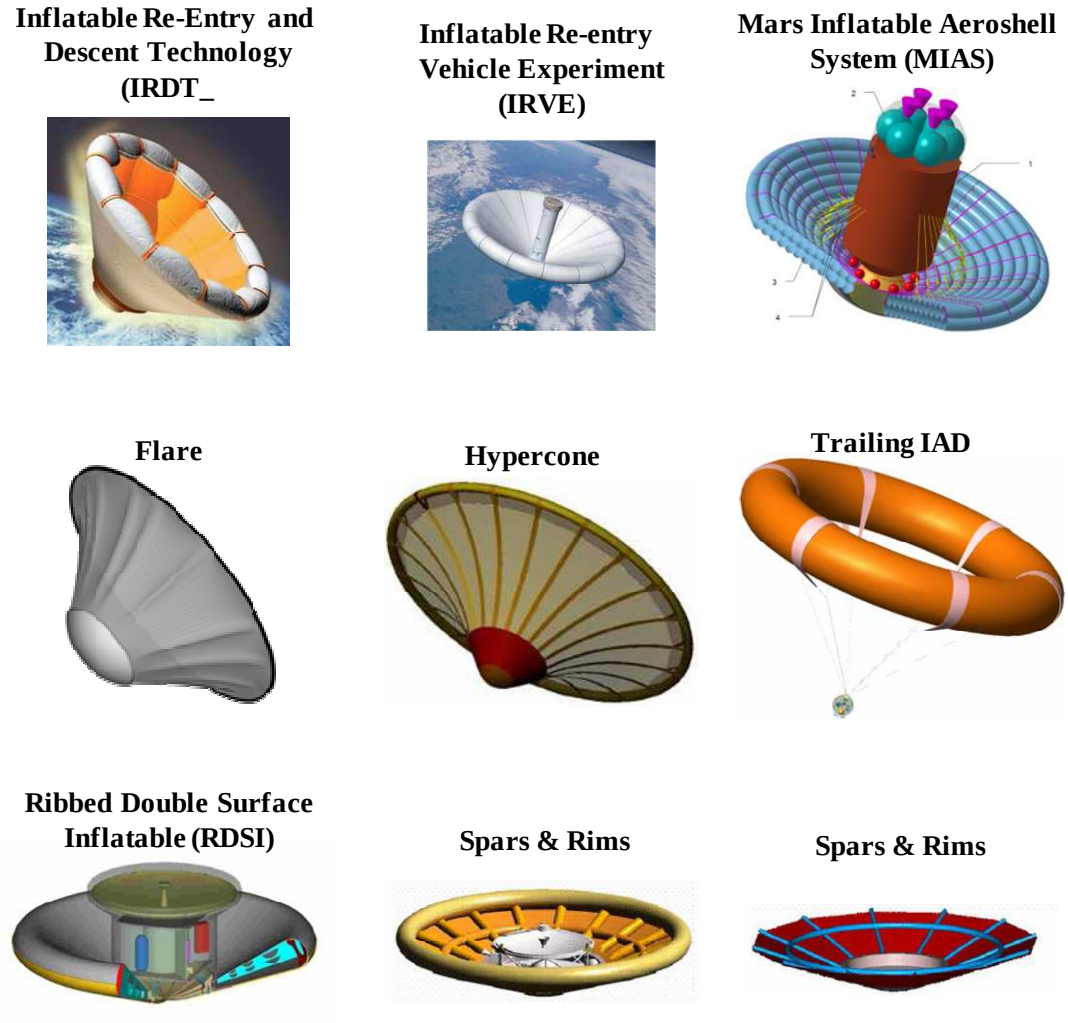

Figure 1. Various IAD concepts.

[†] http://www.astronautix.com/craft/irdt.htm (last visited on May 10, 2011)

Jamshid.A.Samareh@NASA.gov

During system analysis of an IAD design, a large number of concepts are studied. The design is assessed using mission requirements and a set of figures of merit (FOM). System mass is one of the FOMs that is also used for sensitivity analysis and trade studies. The assessment of large number of IAD concepts requires a rapid and accurate parametric approach to estimate masses for various IAD concepts. Parametric mass models are mathematical representations that relate the component mass to the vehicle dimensions and to key mission environmental parameters, such as maximum dynamic pressure. The use of a parametric mass model allows the simultaneous optimization of trajectory and mass sizing parameters. In addition to optimization, these models enable rapid system analysis, sensitivity analysis, and trade study for conceptual level studies. A recent NASA system-analysis project used parametric mass modeling[7–9] for several IAD concepts that were based on the dimensionless parameters that are presented in this paper.

II. Dimensional Analysis

Dimensional analysis is an analytical approach to identifying key dimensionless parameters. These parameters for IAD provide insight into the mass scaling law. Most undergraduate fluid mechanics textbooks include introductory materials on dimensional analysis, and Barenblatt[10] provides a more detailed discussion. The structural mass of an IAD (m) is generally a function of the maximum dynamic pressure ($q_{\max}$) and the projected IAD area (A_{IAD}); the following equation shows an implicit relation for these variables:

$$\Pi = \Pi(m, q_{\max}, A_{\mathrm{IAD}}, g_e) = m^{a_1}\, q_{\max}^{a_2}\, A_{\mathrm{IAD}}^{a_3}\, g_e^{a_4} \tag{1}$$

The term Π is a dimensionless function and g_e is Earth gravity, which is included for the closure. The exponents a_1 through a_4 are determined so that Π is dimensionless. Replacing the units for parameters in Eq. (1) and setting the resulting exponents for each unit to zero yields a system of equations. Solving this system of equations yields

$$\Pi = \left(\frac{m g_e}{A_{\mathrm{IAD}}\, q_{\max}}\right) \tag{2}$$

This equation is modified by dividing it by the aerodynamic drag coefficient so that the first term is similar to the IAD ballistic coefficient; this is also similar to the merit function for isotensoid concepts that was introduced by Anderson et al.[11] The modified version of Eq. (2) is expressed as

$$\bar{m} = \left(\frac{\mathrm{m}\, g_e}{A_{\mathrm{IAD}}\; C_d q_{\max}}\right) = \left(\frac{\mathrm{m}}{A_{\mathrm{IAD}}\; C_d}\right)\left(\frac{g_e}{q_{\max}}\right) = \left(\frac{\mathrm{m}}{A_{\mathrm{IAD}}}\right)\left(\frac{g_e}{q_{\max} C_d}\right) = \frac{\mathrm{m}}{m_{\mathrm{factor}}} \tag{3}$$

The term $\bar{m}$ is the dimensionless mass efficiency parameter that is interpreted either as a ratio of IAD weight to its aerodynamic drag force or as an IAD areal density scaled by dynamic pressure. The term m_{factor} is a scaling mass factor that is defined as $A_{\mathrm{IAD}} C_d q_{\max}/g_e$. An IAD with a lower $\bar{m}$ represents a lower mass concept with a larger frontal area that is capable of withstanding greater maximum dynamic pressure. For example, the $\bar{m}$ for an IAD with an areal density of 4 kg/m^2 and a C_d of 1.5 designed for 5 kPa is 0.0052. Sections IV in this paper explore the dependence of $\bar{m}$ on the IAD geometry, environmental conditions, material properties, and inflation gas properties.

A similar dimensionless analysis of IAD material properties results in a dimensionless parameter for the material tensile yield:

$$\bar{\sigma} = \frac{\sigma}{\rho g_e L}, \tag{4}$$

where σ, ρ, g_e, and L are the material tensile yield, material density, Earth gravity, and characteristic length (assumed to be 1 m in this paper), respectively. The dimensionless parameter $\bar{\sigma}$ is similar to the material breaking length, which is discussed in the next section. For example, the $\bar{\sigma}$ for Kevlar 49 with a yield of 3 GPa and a density of 1440 kg/m^3 is equal to 2.1×10^5. In contrast, the nominal $\bar{\sigma}$ value for aluminum is 2.3×10^4.

Jamshid.A.Samareh@NASA.gov

A similar dimensionless parameter for inflation gas is defined as

$$\bar{G} = \frac{g_e L}{\frac{R}{M}T}, \tag{5}$$

where *R*, *M*, and *T* are the universal gas constant (8314.472 J/kmole·K), the gas molar mass (kg/kmole), and the gas temperature (K), respectively. Concepts that use gases with smaller molecular masses and higher operating temperatures require smaller amount of inflation gas. However, gases with very small molecules (e.g., hydrogen) are prone to leak through gas barriers and negate their lower mass advantage by requiring additional gas to account for leakage. For example, the $\bar{G}$ for an inflation gas with a molecular mass of 22 kg/kmole and an inflation temperature of 0°C is 9.5×10^{-5}.

III. Material Properties

Materials that are used in the construction of an IAD must be flexible, lightweight, and strong. In addition, the materials must withstand tight folding, temperature extremes (e.g., low temperatures during transit and high temperatures during atmospheric entry), abrasion, outgassing, ultraviolet (UV) degradation, vibration, and other harmful environmental elements. Several flight-certified flexible materials are available (e.g., silicone-coated Vectran used for Mars pathfinder airbags). The flexible materials are either polyimide film (e.g., DuPont Kapton® and UBE Upilex®) or synthetic fiber (e.g., DuPont Kevlar® and Kuraray Vectran®). Films have good mechanical and thermal properties, and the inclusion of strong fibers (e.g., glass fiber and nano carbon fiber) can significantly improve their mechanical properties. Synthetic fibers such as Kevlar have their chemical chain molecules highly oriented along the fiber axis, and the strength of the chemical bonds provides high strength. High-performance flexible materials have a much higher specific strength compared with that of metals such as aluminum. Table 1 includes some of the candidate materials for IAD construction along with their nominal properties.

Table 1. Nominal Properties for Candidate IAD Materials

Material	Density (kg/m3)	Elongation at Break (%)	$\overline{\sigma}$	Specific Sterngth (KN-m/kg)	Breaking Strength (km)	Breaking Tenacity (g/Denier)	Tensile strength (Gpa)	Young's modules (Gpa)	Poisson's Ratio	Ref. #
Kapton (Type 100 HN)	1420	72	16583	**163**	**16.6**	**1.84**	0.231	2.5	0.34	1
Kevlar 29 (1500 denier)	1440	3.6	207000	**2031**	**207.0**	23	**2.92**	70.5	0.36	2
Kevlar 49 (1140 denier)	1440	2.4	212400	**2084**	**212.4**	23.6	**3.00**	112.4	0.36	3
M5 (sample)	1700	1.4	237453	**2329**	**237.5**	**26.38**	3.96	271		4
Nomex (Type 430)	1380	30.5	45000	**441**	**45.0**	5	**0.61**	11.45		5
PBO Zylon	1540	3.5	383918	**3766**	**383.9**	**42.66**	5.8	180		6
Spectra 2000 (100 denier)	970	3	350999	**3443**	**351.0**	**39.00**	3.34	124		7
Technora	1390	4.4	220007	**2158**	**220.0**	**24.45**	3	70		8
Upilex-25S	1470	42	36059	**354**	**36.1**	**4.01**	0.52	9.1		9
Vectran (HT)	1410	**4.3**	231346	**2270**	229	**25.44**	3.2	75		10
Aluminium (for reference)	2700		22653	**222**	**22.65**	**2.52**	0.6			
Derived quantities										

All references were last visited on January 4, 2010

1 http://www2.dupont.com/Kapton/en_US/assets/downloads/pdf/summaryofprop.pdf

2 http://www2.dupont.com/Kevlar/en_US/assets/downloads/KEVLAR_Technical_Guide.pdf

3 http://www2.dupont.com/Kevlar/en_US/assets/downloads/KEVLAR_Technical_Guide.pdf

4 http://ammtiac.alionscience.com/pdf/AMPQ9_2ART01.pdf

5 http://www2.dupont.com/Personal_Protection/en_US/assets/downloads/nomex/Nomex_Technical_Guide.pdf

6 http://www.toyobo.co.jp/e/seihin/kc/pbo/Technical_Information_2005.pdf

7 http://www51.honeywell.com/sm/afc/common/documents/3.1_SpectraFiber2000.pdf

8 http://www.matweb.com

Jamshid.A.Samareh@NASA.gov

Terms that are commonly used in the analysis of flexible materials are not common in a typical engineering analysis. Here are the relevant terms used in Table 1:

- *Specific strength* is the material strength divided by the density $\left(\frac{\sigma}{\rho}\right)$, typically measured in $\frac{N-m}{kg}$ or $\left(\frac{m}{s}\right)^2$.
- *Breaking length* is the maximum length of a constant-area column of material that can support its own weight when supported only at the top. It is defined as the specific strength divided by the Earth gravity$\left(\frac{\sigma}{\rho g_e}\right)$. The breaking length unit is typically measured in km.
- *Dimensionless yield parameter* $\bar{\sigma}$ is the ratio of breaking length to the characteristic length, $\bar{\sigma} = \frac{\sigma}{\rho g_e L}$.
- *Denier* is the fiber linear mass density (mass of 9000 m of fiber in g). Sewing thread is around 120–240 deniers. Microfiber is one denier or less. Tex is the international system of unit similar to denier (1 g per 1000 m).
- *Tenacity* is fiber strength expressed as g/denier. It is equal to the breaking length in km divided by 9.

IV. IAD Mass Estimating Approach

Most IAD concepts share a number of common elements: inflatable elements (e.g., toroids, cylinders, and/or spheres), gores (e.g., front cover), and radial straps. This section provides techniques for estimating the mass of IAD elements by using simple engineering approximations and dimensionless parameters. The steps in the mass-estimating process include calculation of 1) the dimensionless geometry parameters, 2) the inflation pressure, 3) the inflation gas mass, 4) the toroid mass, 5) the gore mass, and 6) the radial strap mass. Some steps may be unnecessary for certain IAD concepts. This section also includes calculations for the three IADs that are described in Table 2; these models are referred to as sample IAD models for the remainder of this paper. Some of the input values are similar for the three models; thus, some of the results are suitable for comparison. For example, the drag coefficient is assumed to be 1.5 for all three sample IAD models.

Table 2. Parameters for IAD Samples

Case Number	1	2	3
Model Type	Stacked-Toroid	Tension Cone	Trailing Toroid
Diameter, m	23	15	50
Dynamic Pressure, Pa	3000	1000	200
Number of Toroid	8	1	1
D_t / D_o	Eq. (6)	0.125	0.125
Inner Heatshield Diameter, m	4.5	4.5	4.5
Drag Coefficient	1.5	1.5	1.5
Half-Cone Angle, deg	60	60	60

A. Dimensionless Geometry Parameters

This section presents a set of derivations for the dimensionless geometry parameters for the three IAD concepts that are considered in this paper. As shown in Fig. 2, the IAD geometry parameters are minor diameter (D_t), total IAD diameter (D_o), number of toroids (N), inner heat shield diameter (D_i), and half-cone angle (θ). The rigid section of the heat shield is typically larger than the inner heat-shield diameter. The parameter θ for the trailing IAD must be selected such that the shock from the rigid aeroshell does not contact the IAD surface.

The ratio of minor diameter to the total diameter is a dimensionless parameter that is defined as $\xi_t = \frac{D_t}{D_o}$. The term ξ_t is inversely proportional to the toroid aspect ratio. For tension-cone and trailing types of IADs, the minor diameter is a user-specified parameter. For the stacked toroid type of IAD, the minor diameter is related to the number of toroids in the following manner:

Jamshid.A.Samareh@NASA.gov

$$D_t = \frac{D_o - D_i}{(2N-1)\sin\theta + 1 - \cos\theta} \tag{6}$$

The dimensionless form of Eq. (6) is

$$\xi_t = \frac{D_t}{D_o} = \frac{1-\xi_i}{(2N-1)\sin\theta + 1 - \cos\theta} \tag{7}$$

where ξ_i is $\frac{D_i}{D_o}$. For the sample stacked toroid shown in Table 2, the minor diameter D_t is 1.37 m.

The IAD area ratio (*AR*) is another important dimensionless geometry parameter that is defined as follows.

For a stacked toroid and tension cone,

$$AR = \frac{A_{\text{IAD}}}{A_{\text{Total}}} = \frac{A_{\text{Total}} - A_{\text{heatshield}}}{A_{\text{Total}}} = \frac{\frac{\pi}{4}(D_o^2 - D_i^2)}{\frac{\pi}{4}D_o^2} = 1 - \xi_i^2, \tag{8}$$

For a trailing IAD,

$$AR = \frac{A_{\text{IAD}}}{A_{\text{Total}}} = \frac{A_{\text{Total}} - A_{\text{center}}}{A_{\text{Total}}} = \frac{\frac{\pi}{4}(D_o^2 - (D_o - 2D_t)^2)}{\frac{\pi}{4}D_o^2} = 4\xi_t(1-\xi_t), \tag{9}$$

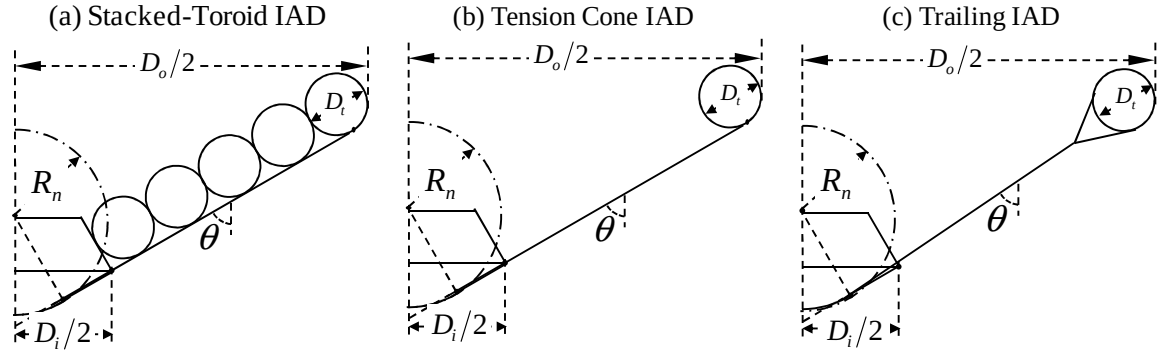

Figure 2. IAD geometries.

The derivations in the reminder of this section are formulated for the stacked toroid; however, the derived dimensionless parameters are valid for the tension cone and the trailing IADs concepts where $N = 1$ and D_t is a user-specified parameter. Toroid mass depends on the dimensionless parameters for the total toroid circumference ($\bar{C}$), the total surface toroid area ($\bar{S}$), and the total toroid volume ($\bar{V}$). These parameters are defined as

$$\bar{C} = \frac{\sum_{i=1}^{N} C_i}{\pi D_o} = N[1 - \xi_t - \xi_t(N-1)\sin\theta] \tag{10}$$

$$\bar{S} = \frac{\sum_{i=1}^{N} S_i}{A_{\text{IAD}}} = \frac{4\pi\xi_t}{AR}\bar{C} \tag{11}$$

$$\bar{V} = \frac{\sum_{i=1}^{N} V_i}{D_t A_{\text{IAD}}} = \frac{\bar{S}}{4} \tag{12}$$

Radial straps connect the heat shield to the IAD. These straps start at the front of the heat shield, loop all the way through the top toroid, and attach to the back of the heat shield. For the trailing IAD, the dimensionless parameter for the length of the radial strap $\bar{L}_r$, is approximated as

Jamshid.A.Samareh@NASA.gov

$$\bar{L}_r = \frac{L_r}{D_o} = \frac{\frac{D_o - D_i - D_t}{2\sin\theta} + (\frac{3\pi}{4}+1)D_t}{D_o} = \left(\frac{1-\xi_i-\xi_t}{2\sin\theta}\right) + \xi_t(\frac{3\pi}{4}+1) \tag{13}$$

For the tension cone IAD, the parameter $\bar{L}_r$ is approximated as

$$\bar{L}_r = \frac{L_r}{D_o} = \frac{1-\xi_i-\xi_t+\cos\theta\xi_t}{2\sin\theta} + \pi\xi_t \tag{14}$$

Similarly for the stacked-toroid IAD concept, $\bar{L}_r$ is approximated as

$$\bar{L}_r = \frac{L_r}{D_o} = \frac{2\left[(N-1)D_t + \frac{\pi}{2}D_t\right]}{D_o} = \xi_t[2(N-1)+\pi] \tag{15}$$

The total surface area of the gore (also referred to as the tension shell) consists of a conical section and an area that covers the top portion of the upper toroid. The dimensionless parameter for the total surface area of the gore is expressed as

$$\bar{A}_{\text{gore}} = \frac{A_{\text{gore}}}{A_{\text{IAD}}} = \frac{\frac{\pi}{4}(D_o^2 - D_i^2)}{\frac{\sin\theta}{A_{\text{IAD}}}} + \frac{\pi^2}{2}(D_o - D_t)D_t = \frac{1}{\sin\theta} + \frac{2\pi\xi_t(1-\xi_t)}{AR} \tag{16}$$

Another critical parameter for the individual gore surface geometry is the maximum local deflected surface curvature[12] r_c, which is defined as (see Fig. 3)

$$r_c^2 = (r_c - \delta)^2 + \left(\frac{c}{2}\right)^2, \quad \delta = \varepsilon c, \quad c = \frac{\pi D_o}{I} \tag{17}$$

where δ is the maximum distance between the undeflected and the deflected gore shape, c is the straight chord distance between two radial straps, ε is the maximum material strain of the gore, and I is the number of radial straps. Rewriting Eq. (17) in a dimensionless form yields

$$\bar{r}_c = \frac{r_c}{D_o} = \frac{\pi}{I}\left(\frac{4\varepsilon^2+1}{8\epsilon}\right) \tag{18}$$

Table 3 shows the dimensionless parameters for the sample IADs that are introduced in Table 2.

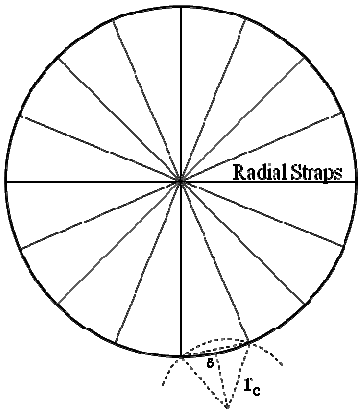

Figure 3. Gore radius of curvature.

Table 3. Dimensionless Geometry Parameters for Sample IADs

Model Number	1	2	3
Toroid Minor Diameter, m	1.37	1.88	6.25
Projected Area Ratio	0.96	0.91	0.44
Dimensionless Toroid Circumference	4.63	0.88	0.88
Dimensionless Toroid Surface Area	3.61	1.51	3.14
Dimensionless Toroid Volume	0.90	0.38	0.79
Dimensionless Gores Max Curvature	0.23	0.23	
Dimensionless Radial Strap Length	1.02	0.76	0.87
Dimensionless Gores Surface Area	1.52	1.91	

B. Inflation Gage Pressure

Toroid mass is strongly dependent on the required inflation pressure. The minimum inflation pressure should be sufficiently high to avoid any in- and out-plane buckling that results from a radial compressive load (F_c) that can be caused by the IAD aerodynamic drag force (F_a).

Jamshid.A.Samareh@NASA.gov

1. Inflation Pressure for Tension Cone and Trailing IADs

The minimum inflation pressure depends on the IAD attachment angles at the payload and toroid locations. Tension-cone design uses gores to attach the payload to the toroid. The gores can undergo significant deformation, resulting in attachment angles at the heat shield and the torus attachment locations that are different from the tension cone angle (see Fig. 4 for key attachment angles). Brown[13] provides a simple approach for calculating the attachment angles. These equations can be further simplified by introducing dimensionless parameters and assuming that the rigid aeroshell and the IAD have similar drag coefficients:

$$\frac{\sin\theta_c}{\sin\theta_d} = \frac{\sin(\theta_t-\theta_d)}{\theta_t-\theta_d}$$
$$\tan\theta_t = -\frac{1}{\tan(2\theta_d)} + \left[\frac{1}{\sin(2\theta_d)}\right]\zeta, \text{ where } \zeta = \frac{AR}{4m_f\xi_t(1-\xi_t)} \quad (19)$$

where $m_f = 1$ for supersonic flows and $m_f = 2$ for hypersonic flows and ζ is the IAD shape parameter. The attachment angles depend only on the dimensionless geometry parameters.

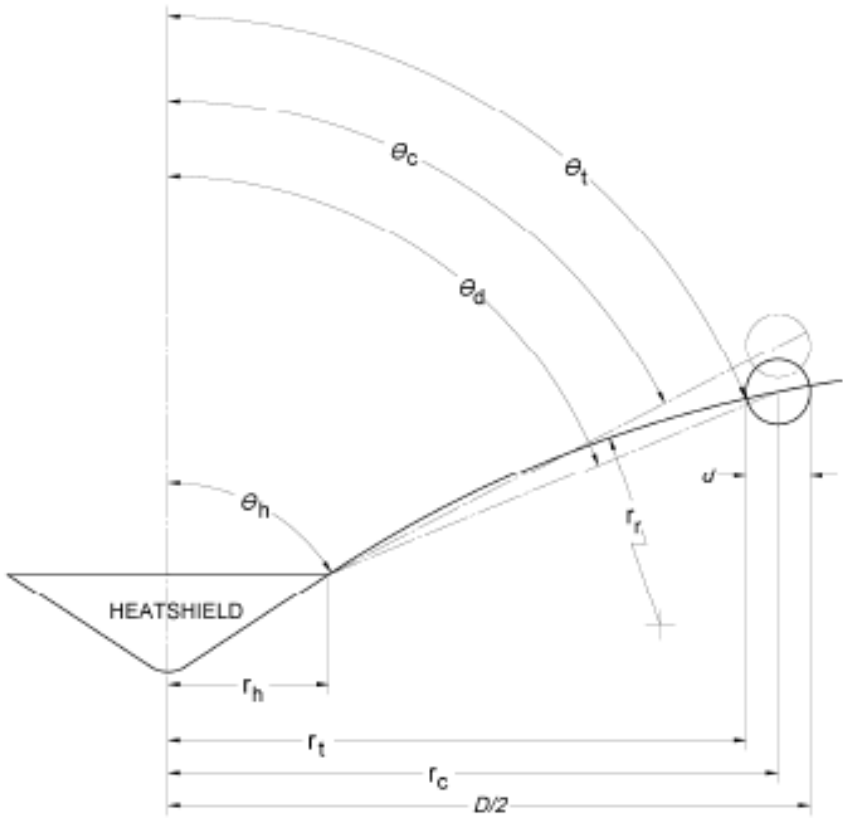

Figure 4. Deflection of radial structure calculated with Brown's approach.

For a given constructed angle (θ_c) and shape parameter (ζ), Eq. (19) is solved for a deflected angle (θ_d) and a torus attachment angle (θ_t). The heat-shield attachment angle (θ_h) is determined from $\theta_h = 2\theta_d - \theta_t$. Figure 5 shows the contours of θ_d/θ_c θ_t/θ_c, and θ_h/θ_c as functions of the shape parameter ζ and the cone angle θ_c. The deflected angle is relatively insensitive to the cone angle and the shape parameter. On the other hand, the torus and the heat-shield attachment angles depend strongly on both ζ and θ_c. For the second sample model, θ_h, θ_d, and θ_t are equal to 59.35, 60, and 60.65 degrees, respectively.

Jamshid.A.Samareh@NASA.gov

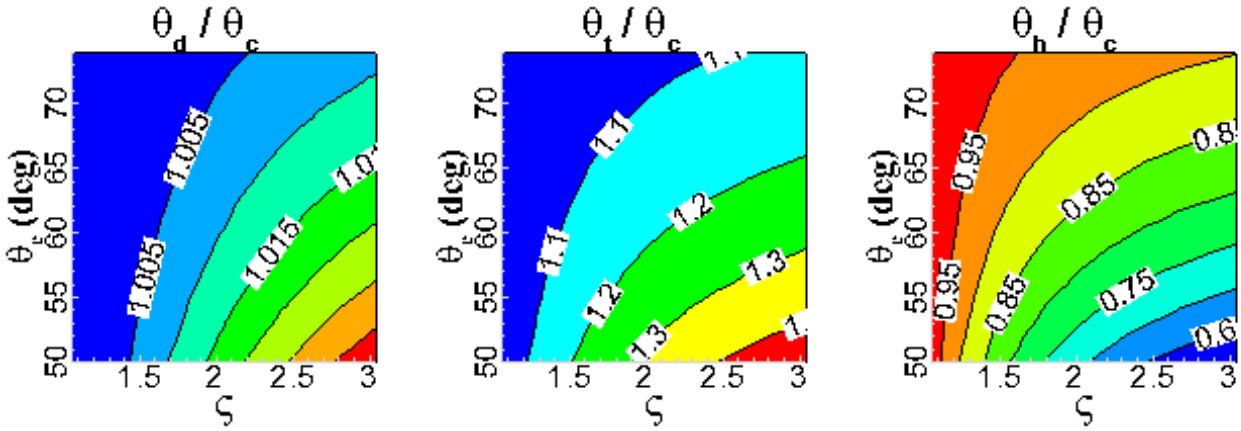

Figure 5. Contours of attachment angles.

Brown[13] suggests that the radial component of tension must be less than the compression reacted by the toroid internal pressure. This results in the following inequality:

$$\frac{\sin\theta_t}{\pi\cos\theta_h}F_a \le \frac{\pi}{4}D_t^2 p \tag{20}$$

Solving Eq. (20) for the minimum inflation pressure ($p_{\min}$) yields

$$p_{\min} = F_a \frac{4\sin\theta_t}{\pi^2 D_t^2 \cos\theta_h} p \tag{21}$$

The estimate in Eq. (20) is two times the value that is obtained by using Brown's formulation.[13] However, the current estimate is consistent with the estimate that is derived by Yamada et al.,[14] which was verified experimentally (Yamada et al. define θ as π/2 – half-cone angle). Kyser[15] provides a similar expression for the minimum inflation pressure for a hypercone ($\theta_t = \pi/2$):

$$p_{\min} = F_a \frac{4}{k\pi^2 D_t^2 \cos\theta_h} \tag{22}$$

where *k* is a factor by which the hoop force during the recovery is reduced below nominal. Equation (21) is also similar to that presented by Clark.[16] Clark incorporated a structural modification (i.e., anti-torque panels) on the backside of the tension cone, which reduced the minimum inflation pressure by a factor of 2.74 below those predicted for models without anti-torque panels. Equation (22) is also valid for trailing torus concepts ($\theta_c = \theta_t = \theta_h = \theta$).

Rewriting Eq. (20) in a dimensionless form yields

$$\bar{p}_{\min} = \frac{p_{\min}}{q_{\max} C_d} = \frac{AR\sin\theta_t}{\pi\,\xi_t^2\cos\theta_h}\eta_p, \tag{23}$$

where η_p is the margin that is included to account for the gas pressure growth allowance due to the low-fidelity nature of the current analysis. The term $\bar{p}_{\min}$ is a dimensionless scaling parameter that depends only on the dimensionless geometry parameters; it is independent of the flow environment. For geometrically similar IAD concepts (i.e., photographically scaled concepts), the scaling parameter $\bar{p}_{\min}$ remains constant and can be used to estimate the minimum inflation pressure based on existing concepts. The term $p_{\min}$ varies linearly with $\bar{p}_{\min}$, the drag coefficient, and the maximum dynamic pressure. If we assume that $\eta_p = 1.25$, then the $\bar{p}_{\min}$ values for the sample IAD models 2 and 3 are equal to 39.63 and 19.30, respectively.

Jamshid.A.Samareh@NASA.gov

2. Inflation Pressure for Stacked Toroid

Brown[13] presents a simple yet effective approach for estimating the minimum inflation pressure for stacked-toroid IAD concepts. This section includes a revised and corrected version of Brown's approach.

Figure 6 shows a simplified stacked toroid model. The virtual work that is done by the structural displacement (δ) that results from aerodynamic forces (F_a) is equal to the volume change (dV) in the gas multiplied by the inflation pressure:

$$F_a \, d\delta = -p_{\min} dV \tag{24}$$

where $\delta = \frac{D_o}{3\tan(\theta)}$. The aeroshell slanted height (h) is defined as

$$h = \frac{D_o}{2\sin(\theta)} \tag{25}$$

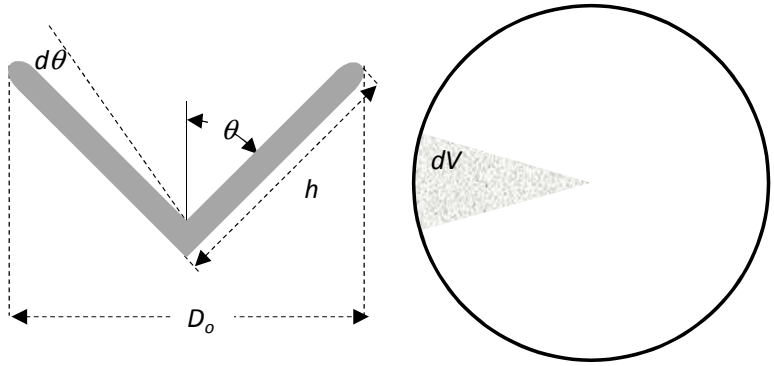

Figure 6. Simplified stacked-toroid model.

Combining the definitions for δ and h yields

$$\delta = \frac{2h}{3}\cos(\theta) \tag{26}$$

Differentiating Eq. (26) with respect to θ results in

$$\frac{d\delta}{d\theta} = \frac{2h}{3}\sin(\theta) = \frac{D_o}{3} \tag{27}$$

The gas volume can be approximated as

$$V = \frac{\pi}{2} D_o h D_t = \pi h^2 D_t \sin(\theta) \tag{28}$$

Differentiating V with respect to θ yields

$$\frac{dV}{d\theta} = \pi h^2 D_t \cos(\theta) = \frac{\pi {D_o}^2 D_t \cos(\theta)}{4\sin^2\theta} \tag{29}$$

Substituting Eqs. (26) and (29) into Eq. (24) yields a definition for the minimum inflation pressure:

$$p_{\min} = F_a \frac{4\tan(\theta)\sin(\theta)}{3\pi D_o D_t} \tag{30}$$

Rewriting $p_{\min}$ in a dimensionless form yields

$$\bar{p}_{\min} = \frac{p_{\min}}{q C_d}\eta_p = \frac{AR\tan(\theta)\sin(\theta)}{3\xi_t}\eta_p \tag{31}$$

Jamshid.A.Samareh@NASA.gov

The dimensionless parameter for the minimum inflation pressure is dependent only on the IAD dimensionless geometry parameters. If we assume that $\eta_p = 1.25$ for sample model 1, then $\bar{p}_{\min}$ equals 10.08.

C. Mass of Inflation Gas and Inflation System

The perfect gas equation ($PV = mRT$) can be used to obtain an expression for the mass of the inflation gas

$$\bar{m}_{\text{gas}} = \frac{m_{\text{gas}} g_e}{q A_{\text{IAD}} C_d} \eta_g = \frac{g_e}{RT} \cdot \frac{p}{q C_d} \cdot \frac{V}{A_{\text{IAD}}} \cdot \eta_g, \quad \bar{m}_{\text{gas}} = \bar{G} \cdot (\bar{p}_{\min} + \Delta \bar{p}_{\text{static}}) \cdot \bar{V} \cdot \xi_t \cdot \bar{D}_o \cdot \eta_g \tag{32}$$

where $\bar{G}$ is the dimensionless gas parameter, $\Delta \bar{p}_{\text{static}} = p_{\text{static}}/(qC_D)$ is the dimensionless static atmospheric pressure, $\bar{V}$ is the dimensionless inflation volume, and $\bar{D}_o$ is the dimensionless IAD overall diameter (D_o/L). The parameter η_g is the growth allowance for the inflation gas that includes leaks and ullage. Equation (32) is valid for any IAD concept. The term $\bar{m}_{\text{gas}}$ is a dimensionless scaling mass parameter for the inflation gas, and this parameter varies linearly with the IAD diameters. The mass scaling parameter depends on the inflation gas properties and the geometry parameters (note that $\bar{p}_{\min}$ also depends only on the geometry parameters). The term $\Delta \bar{p}_{\text{static}}$ becomes critical for applications where a significant atmospheric pressure exists (e.g., at Earth sea level).

If we assume an inflation gas with a molecular weight of 22, an inflation temperature of 0° C, $\eta_g = 1.25$, and $p_{\text{static}} = 100$ Pa, then the calculated $\bar{m}_{\text{gas}}$ for sample models 1, 2, and 3 is 0.001485, 0.003338, and 0.011446, respectively.

Inflation system mass depends on the type and the required amount of inflation gas. Brown et al.[17] provide a review of the available inflation systems for IAD applications. The source of the inflation gas can be compressed gas, liquefied gas, or the products of solid propellant combustion. Selection of the inflation gas depends on the mission duration, the required inflation time, and the environmental conditions during inflation. Exoatmospheric inflation provides ample time for inflation; thus, an inflation system with a lower system mass can be used. Inflation during atmospheric entry demands a rapid inflation; thus, an inflation system with a higher system mass would be required.

The inflation system mass fraction is the mass of the inflation system divided by the mass of the inflation gas. Brown et al.[17] provide the inflation system mass fractions for a number of inflation gasses; these range from liquid hydrogen with system mass fraction of 1 to metal hydride with a mass fraction of 70. Inflation systems that are based on a solid propellant have a system fraction of 1.22. The inflation system mass fraction for the Pathfinder airbags was 3.64.

D. Toroids

The toroid mass depends on the structural concept, the inflation pressure, and the material properties. Possible structural concepts include a combination of a gas barrier with a braided fiber-reinforced fabric, film, or coated fabric. Material availability is another important consideration. In some instances, the minimum required material thickness is smaller than the minimum available material thickness (also referred to as min gage, $t_{\min}$). Hence, the toroid mass is

$$m_{\text{toroid}} = \max\left[\rho \cdot S \cdot t_{\min},\ m_{\text{fully stressed}}\right] \tag{33}$$

where ρ is the material density of the toroid, S is the total surface area of the toroid, and $m_{fully\ stressed}$ is mass of the fully stressed material.

Brown and Sharpless[18] patented a braided airbeam concept that is used here for the braided fiber-reinforced concept. The concept used in this paper has three components: a gas barrier, a braided fiber-reinforced fabric to counter hoop stress, and axial straps to counter in- and out-of-plane buckling. The gas barrier is made of a thin layer of film. Maximum stress and minimum available film thickness determine the total mass of the gas barrier. Brown et al.[19] used a braided tubular beam structure as a deployable wing, and in a later work, Brown et al.[20] used the concept for an inflatable design for the Titan aerocapture. The relation between the total load for the braided fiber-reinforced fabric and the inflation pressure is

$$p_{\min} = \frac{2F_{HL}}{\pi D_t^2\left(1+\frac{1}{\tan^2\beta}\right)} \tag{34}$$

where F_{HL} is the hoop load that results from the inflation pressure and β is the braided fiber bias angle. Fully stressed fiber-reinforced mass is directly proportional to F_{HL} as

$$m_{\text{fiber}} = \rho \frac{F_{\text{hoop load}}}{\sigma} \sum_{i=1}^{N} C_i \tag{35}$$

where C_i is the total circumference of the toroid. Rewriting above equation in a dimensionless form results in

$$\bar{m}_{\text{fiber}} = \frac{1}{\bar{\sigma}} \cdot \left(1 + \frac{1}{\tan^2\beta}\right) \cdot \bar{p}_{\min} \cdot \bar{S} \cdot \frac{\xi_t}{2} \cdot \bar{D}_o \cdot \eta_{\text{fiber}} \tag{36}$$

The first two terms are dependent on the material properties, and the third through the sixth terms are dependent only on the dimensionless geometry parameters. The last term is a combined parameter for seam allowance, factor of safety, margin, and the material knockdown factor that results from an elevated thermal environment:

$$\eta_{\text{fiber}} = \frac{\eta_{\text{seam}}\,\eta_{\text{DFS}}\,\eta_{\text{MGA}}}{\eta_{\text{knockdown}}} \tag{37}$$

If we assume that $\eta_{\text{fiber}} = 4$ and use Kevlar with a yield of 3 GPa and a bias angle of 75 deg, then the calculated $\bar{m}_{\text{fiber}}$ for sample models 1, 2, and 3 is 5.04E-04, 1.13E-03, and 3.82E-03, respectively.

Axial straps are used to counter both in-plane and out-of-plane buckling. The axial stiffness must resist the axial load in the toroid as

$$\frac{\pi}{4} D_t^2 p_{min} = \sigma t \pi D_t \tag{38}$$

The dimensionless mass parameter for the axial straps is expressed as

$$\bar{m}_{\text{axial}} = \frac{1}{\bar{\sigma}} \cdot \bar{p}_{\min} \cdot \bar{S} \cdot \frac{\xi_t}{4} \cdot \bar{D}_o \cdot \eta_{\text{axial}}\,. \tag{39}$$

The term η_{axial} is similar to η_{fiber}. If we assume that $\eta_{\text{axial}} = 4$ and use Kevlar with a yield of 3 GPa, then the calculated $\bar{m}_{\text{axial}}$ for sample models 1, 2, and 3 is 2.35E-04, 5.28E-04, and 1.78E-03, respectively.

Film and coated fabric concepts are alternatives to the braided fiber-reinforced concept. Roark and Budynas[21] provide a linear expression for the maximum stress for toroidal concepts as

$$\sigma_{\max} = \frac{pD_t}{4t}\left[\frac{D - D_t - \frac{D_t}{2}}{\frac{D-D_t}{2} - \frac{D_t}{2}}\right] = \frac{pD_t}{4t}\left[2 + \frac{D_t}{D-2D_t}\right], \tag{40}$$

where D is the outside diameter (D_o) of the toroid for IADs with a single toroid and the diameter of the smallest toroid for a stacked-toroid concept. Lindell et al.[22] provides a similar relation. In addition, Rossettos and Sanders[23] and Sanders and Liepins[24] show that the resultant maximum stress is similar to that obtained from the nonlinear membrane analysis. They show that the results from linear analysis follow very closely the values that are obtained from linear bending and nonlinear membrane theory. The dimensionless mass parameter for coated fabric and film is expressed as

$$\bar{m}_{\text{toroid}} = \frac{1}{\bar{\sigma}} \cdot \bar{p}_{\min} \cdot \bar{S} \cdot \frac{\xi_t(2-3\xi_t)}{4(\xi_D - 2\xi_t)} \cdot \bar{D}_o \cdot \eta_{\text{toroid}} \tag{41}$$

where $\xi_D = 1$ for an IAD with a single toroid and $\xi_D = \xi_i + 2\xi_t$ for a stacked toroid concept. The first term is the dimensionless material property; the rest of the parameters are dependent on the IAD geometry. The dimensionless mass for coated fabric must be augmented by the mass for the coating material. Equation (41) is also applicable for

estimating the mass of a fully stressed gas barrier for a fiber-reinforced fabric concept: the right-hand side of the equation must be multiplied by the ratio of the gap in braided fiber-reinforced fabric to the minor toroid diameter. If we assume that $\eta_{\text{toroid}} = 4$ and use Kevlar with a yield of 3 GPa, then the calculated value of $\bar{m}_{\text{toroid}}$ for sample model 1 is 1 5.41E-5; if we use Upilex with a yield of 0.5 GPa, then the calculated value of $\bar{m}_{\text{toroid}}$ for the same sample model 1 is 3.32E-3. Tables 4 and 5 provide additional details.

E. Radial Straps

The radial straps carry the IAD aerodynamic load and connect the heat shield to the IAD. The straps start at front of the heat shield, loop all the way around the top of the toroid, and attach to the back of the heat shield. The tension in the straps is a function of IAD drag as

$$T = \frac{D_{\text{IAD}}}{\cos\theta_h} = \sigma A_r \tag{42}$$

where D_{IAD} is the IAD drag force, θ_h is the attachment angle at the heat shield, and A_r is the radial-strap cross-sectional area. The dimensionless mass parameter for radial straps is expressed as

$$\bar{m}_{\text{radial}} = \frac{1}{\bar{\sigma}} \cdot \frac{\bar{L}_r}{\cos\theta_h} \cdot \bar{D}_o \cdot \eta_{\text{radial}} \tag{43}$$

where $\bar{L}_r$ is the dimensionless length for the radial straps. For stacked-toroid and trailing IADs, θ_h is the cone angle (θ_c). If we assume that $\eta_{\text{radial}} = 4$ and use Kevlar with a yield of 3 GPa, then the calculated $\bar{m}_{\text{radial}}$ for sample models 1, 2, and 3 is 8.86E-04, 4.22E-04, and 1.64E-03, respectively.

F. Gores

Clark[16] provides a detailed discussion of relevant tension shell theory and shape trade space. Gores serve two purposes: they act as a gas barrier and withstand local surface pressure. We assume that the radial straps carry the drag forces and the associated payload deceleration loads. Stresses in gores are defined as

$$\frac{N_\theta}{r_\theta} + \frac{N_\phi}{r_\phi} = p_s \tag{44}$$

where p_s is the gore surface pressure, N_θ and N_ϕ are gore linear stresses, and r_θ and r_ϕ are the radii of curvature in the θ and ϕ directions, respectively (see Fig. 7). For cones, r_θ approaches infinity, and Eq. (44) reduces to

$$N_\theta = r_\theta p_s \Longrightarrow \sigma t = r_c p_s \tag{45}$$

where σ is the maximum material yield stress, t is the gore thickness, and r_c is the maximum radius of curvature of the gore (see section IV.a for the derivation). The dimensionless parameter for the fully stressed mass is expressed as

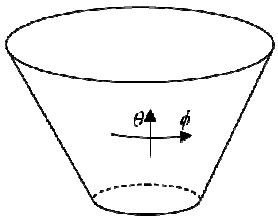

Figure 7. Gore geometry.

$$\bar{m}_{\text{gores}} = \frac{1}{\bar{\sigma}} \cdot \bar{r}_c \cdot \bar{A}_{\text{gores}} \cdot \bar{D}_o \cdot \eta_{\text{gores}} \tag{46}$$

The terms $\bar{r}_c$ and $\bar{A}_{\text{gores}}$ are the dimensionless maximum curvature and the dimensionless parameter for the surface area of the gore (see IV.a for definitions), respectively. Similar to other dimensionless mass parameters, the dimensionless parameter for the gore mass depends only on the dimensionless material parameters and the dimensionless geometry parameters. Similar to toroid mass, the gore mass must be equal to or greater than the mass of gores that are made of material with the minimum available thickness. If we assume $\eta_{\text{gores}} = 4$ and use Upilex with yield of 0.5 GPa, then the calculated $\bar{m}_{\text{gores}}$ for sample models 1 and 2 is 9.61E-04 and 7.87E-04, respectively.

Jamshid.A.Samareh@NASA.gov

V. Results

This section provides sample mass calculations for nine IAD models. These models are not intended to be used as optimal reference IAD designs. Estimating IAD mass requires roughly 50 input parameters, including environmental conditions, geometry parameters, material properties, inflation gas properties, factors of safety, margins, material knockdown factors, and many others. These input parameters must be judiciously selected to reflect a particular design and technology readiness level. These nine cases have been selected to represent the combination of IAD concepts (stacked toroid, tension cone, and trailing IAD shown in Table 1) and toroid concepts (fiber-reinforced fabric, coated fabric, and film).

Tables 1 and 4 provide the input parameters that have been used in this section. Table 5 shows the results for the nine selected sample cases. The first three columns show results for fiber-reinforced fabric for a stacked toroid, a tension cone, and a trailing IAD. Columns 4 through 6 provide the same results for a coated fabric, and columns 7 through 9 provide the same results for film. Figure 8 shows the results for cases 1 through 3 using randomly selected diameter values between 6 and 40 m and dynamic pressure values between 20 and 3000 Pa. As expected from the derived equations in this paper, IAD areal density varied linearly with the product of dynamic pressure and IAD diameter. Readers should note that cases 1 through 3 have exactly the same common input parameters, although the IAD concepts differ. Figure 8 also shows the results from Anderson et al.[11] report. The current sample results are bounded by Anderson's results. The models that were used by Anderson et al. include an attached isotensoid model and a trailing isotensoid model, which differ significantly from the models that are used in this work.

The Mars EDL-SA study that was conducted by NASA in FY 2009–2010 examined eight unique exploration-class architectures that included elements such as a rigid mid-*L/D* aeroshell, a lifting hypersonic inflatable decelerator, a drag supersonic inflatable decelerator, a lifting supersonic inflatable decelerator implemented with a skirt, and subsonic/supersonic retro-propulsion. The parametric models that were used in the EDL-SA study relate the component mass to the vehicle dimensions and key environmental parameters, such as maximum deceleration and total heat load. The use of a parametric mass model allows the simultaneous optimization of trajectory and mass sizing parameters. The Mars EDL-SA project used technique described in section IV to estimate the masses of the inflatable concepts that were examined in the analysis.[7–9] The EDL-SA results compared well with independent high-fidelity finite-element analyses.[25]

Table 4. Common Input Parameters

	Common Parameteres				
Environment Parameters	2	Hypersonic Regim	Geometry	4.5	Inner Heatshield Diameter, m
	1.5	Drag Coefficient		60	Cone Angle, deg
	100	Static Pressure, Pa		18	Number of Radial Straps
	0	Inflation Gas Temperature, C	Gas	22	Inflation Gas Molecular Weight
	1	Gores Ps / (qCd)		0.3	Inflation System Mass Fraction
Material Properties	3E+09	Radial Straps Yield, Pa	Factor of Saftey, Margins, and Knock Down Factors	1.05	Gores Seams Margin
	1440	Radial Straps Material Density, kg/m^3		4	Gores DFS for Loads
	2.54E-05	Toroid Minimum Thickness, m		1	Gores Knock Down
	75	Toroid Fiber Reinforced Bias Angle, deg		4	Toroid Fiber Reinforced DFS
	0.05	Toroid Fiber Gap Ratio (gap over minor diameter)		1	Toroid Fiber Reinforced MGA
	0.5	Toroid Fiber Adhesive or Coating Mass Fraction		1	Toroid Fiber Reinforced Knock Down
	5E+08	Toroid Gas Barrier Material Yield, Pa		4	Toroid Gas Barrier DFS
	1470	Toroid Gas Barrier Material Density, kg/m^3		1	Toroid Gas Barrier knockdown factor
	5.08E-05	Toroid Gas Barrier Minimum Thickness, m		4	Toroid Axial Straps DFS
	1.05	Toroid Gas Barrier Seam Allowance + MGA		1	Toroid Axial Straps MGA
	3E+09	Toroid Axial Straps Material Yield, Pa		1	Toroid Axial Straps Knock Down
	1440	Toroid Axial Straps Material Density, kg/m^3		1.25	Inflation Gas Pressure Margin
	5E+08	Gores Material Yield, Pa		1.25	Inflation Gas MGA
	1470	Gores Material Density, kg/m^3		4	Radial Straps DFS
	10	Gores Material Max Strain, %		1	Radial Straps MGA
	1.4732E-05	Gores Minimum Thickness, m		1	Radial Straps Knock Down

Table 5. Results for Nine Sample Cases

Fiber Reinforced Fabric			Coated Fabric			Film			Comments
Case 1	Case 2	Case 3	Case 4	Case 5	Case 6	Case 7	Case 8	Case 9	
ST*	TC*	TI*	ST*	TC*	TI*	ST*	TC*	TI*	Concepts
23	15	50	23	15	50	23	15	50	D_o
8	8	8	8	8	8	8	8	8	N or $1/\xi_t$
3000	1000	200	3000	1000	200	3000	1000	200	q_{max}
3E+09	3E+09	3E+09	3E+09	3E+09	3E+09	5E+08	5E+08	5E+08	Toroid Yield, PA
1440	1440	1440	1440	1440	1440	1470	1470	1470	Toroid Material Density, kg/m^3
183290	24589	26270	183290	24589	26270	183290	24589	26270	Mass Factor (Eq. 3), kg
1039	**221**	**888**	**885**	**188**	**617**	**1368**	**325**	**1112**	Total Mass (Eq. 3), kg
									Dimensionless Parameteres
5.38E-03	8.55E-03	3.21E-02	4.59E-03	7.27E-03	2.23E-02	7.09E-03	1.26E-02	4.02E-02	Total Mass
4.63	0.88	0.88	4.63	0.88	0.88	4.63	0.88	0.88	Toroid Circumference (Eq. 10)
3.61	1.51	3.14	3.61	1.51	3.14	3.61	1.51	3.14	Toroid Surface Area (Eq. 11)
0.90	0.38	0.79	0.90	0.38	0.79	0.90	0.38	0.79	Toroid Volume (Eq. 12)
1.02	0.76	0.87	1.02	0.76	0.87	1.02	0.76	0.87	Radial Strap Length (Eq. 13)
1.52	1.91	2.73	1.52	1.91	2.73	1.52	1.91	2.73	Gores Surface Area (Eq. 16)
0.23	0.23	0.23	0.23	0.23	0.23	0.23	0.23	0.23	Gores Max Curvature (Eq. 18)
10.08	39.63	19.30	10.08	39.63	19.30	10.08	39.63	19.30	Inflation Pressure (Eqs. 23 & 31)
1.48E-03	3.34E-03	1.14E-02	1.48E-03	3.34E-03	1.14E-02	1.48E-03	3.34E-03	1.14E-02	Inflation Gas Mass (Eq. 32)
4.45E-04	1.00E-03	3.43E-03	4.45E-04	1.00E-03	3.43E-03	4.45E-04	1.00E-03	3.43E-03	Inflation System Mass
5.04E-04	1.13E-03	3.82E-03	5.41E-04	1.14E-03	3.87E-03	3.32E-03	7.01E-03	2.37E-02	Toroid Fiber/Film Mass (Eqs. 35 & 41)
2.52E-04	5.66E-04	1.91E-03	2.71E-04	5.72E-04	1.93E-03				Toroid Adhesive/Coating Mass
6.17E-04	7.75E-04	8.06E-03							Toroid Gas Barrier Mass (Eqs. 33 & 41)
2.35E-04	5.28E-04	1.78E-03							Toroid Axial Straps Mass (Eq. 39)
8.86E-04	4.22E-04	1.64E-03	8.86E-04	4.22E-04	1.64E-03	8.86E-04	4.22E-04	1.64E-03	Radial Straps Mass (Eq. 43)
9.61E-04	7.87E-04		9.61E-04	7.87E-04		9.61E-04	7.87E-04		Gores Mass (Eq. 46)
0.05	0.05	0.05	0.05	0.05	0.05	0.05	0.05	0.05	Misc Mass (5% of Total mass)

*ST: Stacked Toroid. TC Tension Cone, TI: Trailing IAD

Jamshid.A.Samareh@NASA.gov

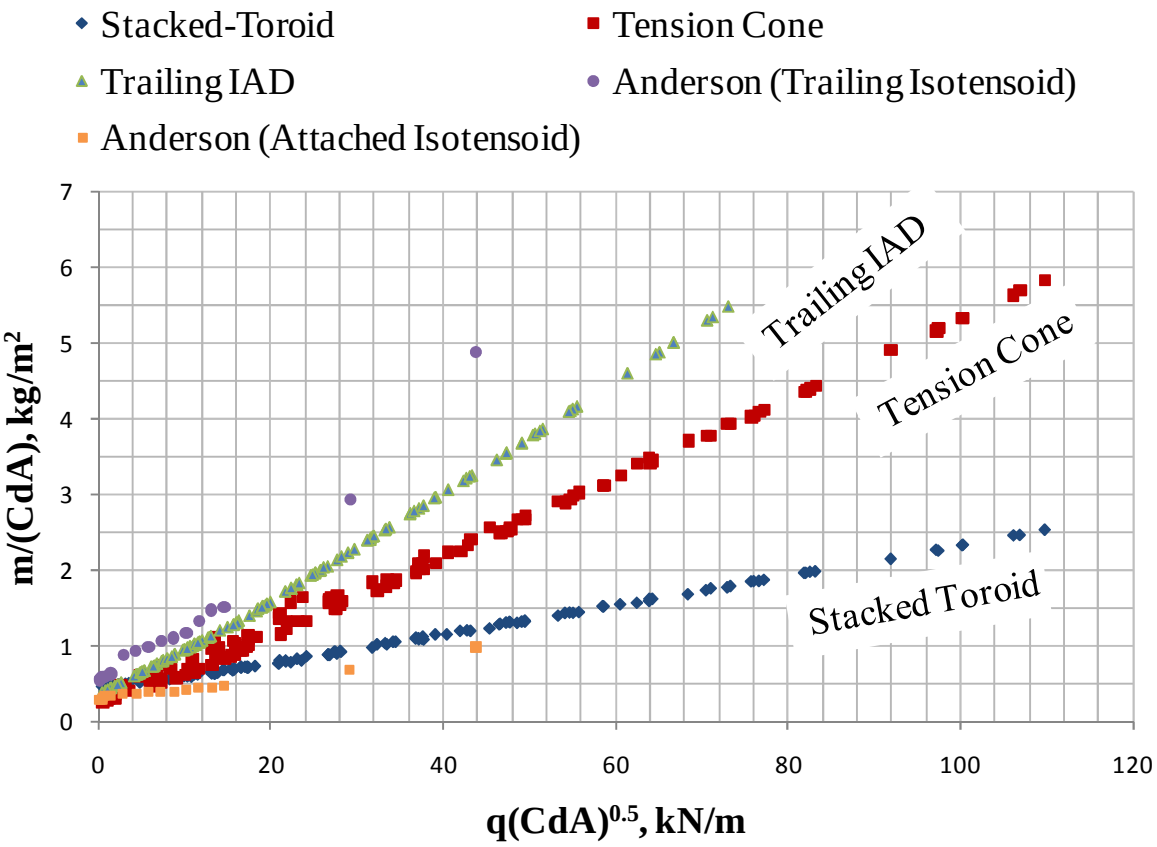

Figure 8. Plot of Anderson's merit function for sample cases 1 through 3.

VI. Summary

This paper provides a set of dimensionless parameters for inflation pressure, mass of inflation gas, and mass of flexible material. These parameters enable the scaling of an inflatable concept with respect to geometry-sizing parameters, environmental conditions, inflation gas properties, and mass growth allowance. The approach is applicable for tension cone, hypercone, stacked toroid, and trailing types of inflatable aerodynamic decelerators. The results are presented for nine sample models. To identify the important design parameters, 129 models were randomly generated, and their masses were estimated. The results indicate that the areal density for inflatable aerodynamic decelerators varies linearly with the product of maximum dynamic pressure and diameter. The results for the stacked toroid type of IAD compared well with two independent sets of high-fidelity finite-element analyses.

Jamshid.A.Samareh@NASA.gov

Acknowledgments

The author would like to thank Glenn Brown of HDT Engineering Services for verifying the revised derivation for the minimum inflation pressure for the stacked-toroid concept and Reuben Rohrschneider of Ball Aerospace for suggesting a simpler version of Eq. (19).

References

[1]Braun, R. and Manning, R., "Mars Exploration Entry, Descent, and Landing Challenges," *Journal of Spacecraft and Rockets*, Vol. 44, No. 2, 2007, pp. 310–323.
[2]Rohrschneider , R. and Braun, R., "Survey of Ballute Technology for Aerocapture," *Journal of Spacecraft and Rockets*, Vol. 44 No. 1, 2007, pp. 10–23.
[3]Reza, S., Kustas, F., Willcockson, W., Songer, J., Makowski, K., and Brown, G., "Aerocapture Inflatable Decelerator (AID) for Planetary Entry," AIAA-2007-2516, may 2007.
[4]Hughes, S. J., Dillman, R. A., Starr, B. R., Stephan, R. A., Lindell, M. C., Player, C. J., and Cheatwood, F. M., "Inflatable Re-entry Vehicle Experiment (IRVE) Design Overview," AIAA 2005-1636, May 2005.
[5]Wilde, D. and Walther, S., "Flight Test and ISS Application of the Inflatable Reentry and Descent Technology (IRDT)," *Acta Astronautica*, Vol. 51, No. 1–9, 2002, pp. 83–88.
[6]Yamada, K., Akita, D., Sato, E., Narumi, R., and Abe, T., "Flare-Type Membrane Aeroshell Flight Test at Free Drop from a Balloon," *Journal of Spacecraft and Rockets*, Vol. 46, No. 3, 2009, pp. 606–614.
[7]Samareh, J. A. and Komar, D. R., "Parametric Mass Modeling for Mars Entry, Descent, and Landing System Analysis Study," AIAA Paper 2011-1038, Jan 2011.
[8]Dwyer Cianciolo, A. M., Davis, J. L., Komar, D. R., Munk, M. M., Samareh, J. A., Powell, R. W., Shidner, J. D., Stanley, D. O., W., A. W., Kinney, D. J., McGuire, M. K., Arnold, J. O., Howard, A. R., Sostaric, R. R., Studak, J. W., Zumwalt, C. H., Llama, E. G., Casoliva, J., Ivanov, M. C.; Clark, I., and Sengupta, A., "Entry, Descent and Landing Systems Analysis Study: Phase 1 Report," NASA/TM-2010-216720, March 2010.
[9]Dwyer Ciancolo, A., Davis, J., Engelund, W, Komar, D. R., Queen, E. M., Samareh, J. A., Way, D. W., Zang, T. A., Murch, J. G., Krizan, S. A., Olds, A. D., Powell, R. W., Shidner, J. D., Kinney, D. J., McGuire, M. K., Arnold, J. O., Covington, M. A., Sostaric, R. R., Zumwalt, C. H., and Llama, E. G.," Entry, Descent and Landing Systems Analysis Study: Phase 2 Report on Exploration Feed-Forward Systems," NASA-TM-2011-217055, March 2011.
[10]Barenblatt, G. I., *Dimensional Analysis*, Gordon and Breach Science Publisher, New York, 1987.
[11]Anderson, M. S., Bohon, H. L., and Mikulus, M. M., "A Structural Merit Function for Aerodynamic Decelerators," NASA-TN-D-5535, November 1969.
[12]Rohrschneider, R. R. and Brown, G. J., "Performance and Configuration Study of Deployable High-Mass Mars Entry Systems: Final Report," NASA Contract Report, NNL08AA34C, April 15, 2010.
[13]Brown, G. J., "Estimating Minimum Inflation Pressure for Inflatable Aerodynamic Decelerators," AIAA-2009-2970 (revised on June 8, 2009).
[14]Yamada, K., Kimura, Y., Akita, D., Abe, T., Suzuki, K., Imamura, O., Koyama, M., and Hayashi, A. K., "Study on Low-Ballistic-Coefficient Atmospheric-Entry Technology Using Flexible Aeroshell," *Transactions of Space Technology Japan*, Vol. 7, No. 26, 2009, pp. 1–7.
[15]Kyser, A. C., "Deployment Mechanics for an Inflatable Tension-Cone Decelerator," NASA-CR-929, November 1967.
[16]Clark, I., "Aerodynamic Design, Analysis, and Validation of a Supersonic Inflatable Decelerator," Ph.D. Thesis, Department of Aerospace Engineering, Georgia Institute of Technology, Atlanta, GA, 2009.
[17]Brown, G. J., Epp, C., Graves, C., Lingard, S., Darley, M., and Jordan, K., "Hypercone Inflatable Supersonic Decelerator," AIAA-2003-2167, May 2003.
[18]Brown, G. J. and Sharpless, G. C., "Braided Airbeam Structure," United States Patent 5735083, April 7, 1998.
[19]Brown, G. J., Haggard, R., and Norton, B., "Inflatable Structures for Deployable Wings," AIAA-2001-2068, June 2001.
[20]Brown, G. J. and Richardson, E., "Minimum-Mass Design for Titan Aerocapture," AIAA-2005-1637, May 2005.
[21]Roark, W. C. and Budynas, R. G., *Roark's Formulas for Stress and Strain*, McGraw-Hill, 2002.
[22]Lindell, M., Hughes, S., Dixon, M., and Willey, C., "Structural Analysis and Testing of the Inflatable Re-Entry Vehicle Experiment (IRVE)," AIAA-2006-1699, May 2006.
[23]Rossettos, J. N. and Sanders, J. L., "Toroidal Shells Under Internal Pressure in the Transition Range," *AIAA Journal*, Vol. 3, No. 10, October 1965, pp. 1901–1909.
[24]Sanders, J. L. and Liepins, A. A., "Toroidal Membrane Under Internal Pressure," *AIAA Journal*, Vol. 1, No. 9, September 1963, pp. 2105–2110.
[25]Sheta, E., Venugopalan, V., Tan, X. G., Liever, P. A., and Habchi, S. D., "Aero-Structural Assessment of an Inflatable Aerodynamic Decelerator," NASA/CR–2010-216731, August 2010.

Jamshid.A.Samareh@NASA.gov